2018

Theoretical and Experimental Evaluation of Microchannel Condensers Applied to Household Refrigerators

Renata Soares Rametta
Embraco S.A., renata.s.rametta@embraco.com

Joel Boeng
Federal University of Santa Catarina, Brazil, joel@polo.ufsc.br

Joel Boeng
melo@polo.ufsc.br

Theoretical and Experimental Evaluation of Microchannel Condensers Applied to Household Refrigerators

Renata S. RAMETTA, Joel BOENG, Cláudio MELO*

POLO – Research Laboratories for Emerging Technologies in Cooling and Thermophysics
Department of Mechanical Engineering, Federal University of Santa Catarina
88040-900, Florianópolis, SC, Brazil, +55 48 3721 7900

* Corresponding Author: melo@polo.ufsc.br

ABSTRACT

Microchannel heat exchangers, although widely used in the automotive and air-conditioning industry, are not usually used in domestic refrigeration especially because of its prohibitive cost. However, with the recent manufacturing processes advance, these heat exchangers have become a tangible option, mainly due to their compact design and high heat transfer rate per unit of volume. This work aims to theoretically and experimentally evaluate the impact of the use of forced-draft microchannel condensers on a specific household refrigerator model. In this context, a mathematical model was developed to predict the heat transfer rate and the air-side pressure drop of microchannel heat exchangers. This model was incorporated to an existing simulation platform for household refrigerators, which allowed correlating the geometry of the heat exchanger with the energy consumption of the appliance. Experiments were carried out in a wind tunnel and in a climatic chamber, which allowed validating both condenser and refrigerator mathematical models. It was observed that the prediction of the heat transfer rate and the air-side pressure drop in the condenser respectively remained within ±10% and ±20% error bands. It was also found that energy consumption was predicted with maximum errors of ±3.5%. Sensitivity analyzes were also performed, pointing to a 13% drop in the energy consumption of the refrigerator with the use of a microchannel condenser with 20 passes, 200mm high, 180mm wide, 72mm deep, 200 fins per meter and 46 rectangular channels of 1.2mm of hydraulic diameter.

1. INTRODUCTION

Forced-draft condensers are regularly used in household refrigerators due to the enhanced heat transfer rate. Therefore, an airflow system, comprised by a fan, by the condenser itself and by inlet and outlet ducts, must be designed and integrated into the compressor niche. It is then evident that the condenser shall be compact and present low impedance to the air flow.

Microchannel condensers are commonly used in air conditioning systems and automotive radiators due to its high heat transfer rates per unit of volume. However, such technology was not so far used in domestic refrigeration due to its high cost. At present, cost is not prohibitive any longer due to recent technological advances in the manufacturing process. Moreover, an additional microchannel benefit is the potential reduction of the refrigerant charge, particularly relevant when hydrocarbons are used. In contrast, such heat exchangers suffer from an irregular refrigerant distribution in the microchannel ports and greater pressure drops, both on the refrigerant and air sides.

Many studies in the literature focus on microchannel heat exchangers, especially for air conditioners and automotive radiators. Park and Hrnjak (2008) observed a 13.1% raise in the Coefficient of Performance (COP) of a residential air conditioning system when the regular fin-on-tube condenser was replaced by a microchannel condenser with vertical distributors. In addition, the authors observed a drop of 2.5°C in the condensing temperature, a reduction in the refrigerant side pressure drop from 166kPa to 57kPa and a 9.2% reduction in the refrigerant charge.

The irregular distribution of refrigerant in microchannel heat exchangers with vertical distributors is due to the distributor geometry, the non-uniformity airflow and the condenser positioning. This subject has been studied numerically and experimentally by Huang et al. (2014), which showed that gravity has a striking effect on the flow distribution in a microchannel condenser of an automotive air conditioning system fed by a vertical distributor. Shao

et al. (2009), in turn, developed a mathematical model to simulate the behavior of microchannel condensers in serpentine format and estimated that, in these heat exchangers, the refrigerant charge is half of that found in similar heat exchangers but with vertical distributors.

Indeed, irregular distribution of refrigerant is an intrinsic problem for long and vertical distributors, rarely occurring in microchannel condensers with short and horizontal distributors, in serpentine format. In contrast, the latter are subject to a higher internal pressure drop due to the non-splitted flow and to the longer condenser length.

In this context, the present work aims to model, test and apply forced-draft microchannels condensers in a specific domestic refrigerator. To this end, numerical analysis was performed to optimize the condenser, using the refrigerator energy consumption as an outcome. Experiments were also performed, in a wind tunnel to characterize the heat exchanger and in a climatic chamber to characterize the refrigerator.

2. EXPERIMENTAL APPROACH

The experimental work was divided into two phases: (i) thermo-hydraulic performance evaluation of several microchannel condensers design in a wind tunnel and (ii) energy consumption evaluation of a unique domestic refrigerator mounted with the most promising condenser design, in a climatic chamber.

2.1 Samples

The condensers used in this work are essentially formed by two small distributors placed horizontally at the inlet and outlet of a coil formed by parallel microchannels and by louver-type fins, as shown in Figure 1. Two types of cross sections were tested: the first with 31 parallel circular channels, with diameter of 0.64mm, and the second with 12 parallel rectangular channels, with hydraulic diameter of 1.24mm. Four heat exchangers were selected for each cross section, based on the available space inside the compressor niche, totaling 8 samples. The fin density and the condenser depth were fixed for all samples.

Table 1 shows the samples geometry. The circular section condensers are the odd and the rectangular section ones the even. Two extra samples (#9 and #10), both with 7 parallel rectangular channels with hydraulic diameter of 1.2 mm, were also evaluated. It must be noted that these samples differ substantially from the others, especially in depth and fin density.

Figure 1: Microchannel condensers

2.2 Experimental apparatus

The condensers were tested in a wind tunnel, designed and built according to the ASHRAE 37 (1987), 41.2 (1988) and 51 (1999) Standards. The apparatus is basically comprised by two independent circuits: air and water sides.

The tests were carried out with volumetric airflow rates between 50 and 140 m³/h, which is typical range for domestic refrigeration. The air temperature at the wind tunnel inlet was kept constant at 21°C by an air conditioning system and an electrical heater. The water inlet temperature was kept constant at 40°C by a thermostatic bath and the water mass flow was controlled in order to maintain the inlet and outlet water temperatures difference at 3°C. The volumetric airflow rate was measured by a set of nozzles. All variables were acquired in real time, with reading intervals less than 1s. A steady state criterion, based on predetermined values of standard deviation for each variable, was developed and used during the tests.

Table 1: Samples geometry

Samples	#1 / #2	#3 / #4	#5 / #6	#7 / #8	#9	#10
Number of passes [-]	10	12	14	18	20	18
Passes pitch [mm]	9.1	9.1	9.1	9.1	10	10
Height [mm]	83.8	101.6	119.4	157.5	200	180
Width [mm]	91.7	117.1	142.5	167.9	170	200
Depth [mm]	31.8	31.8	31.8	31.8	12	12
Coil thickness [mm]	1.5	1.5	1.5	1.5	2	2
Fin height [mm]	7.6	7.6	7.6	7.6	8	8
Fin density [fins/m]	1000	1000	1000	1000	700	700
Fin thickness [mm]	0.1	0.1	0.1	0.1	0.1	0.1

2.3 Data reduction

2.3.1 Heat transfer rate

An energy balance on the air or water side provides the respective heat transfer rate. The declared heat transfer rate is the arithmetic mean of the heat transfer calculated on both sides, since these values do not differ by more than ±10%.

The overall thermal conductance coefficient (UA) was calculated by the ε-NTU method, for heat exchangers with mixed C_{min} and unmixed C_{max}, where C is the thermal capacity (Incropera et al., 2007). The heat transfer rate was also expressed by the dimensionless parameter *j*, introduced by Colburn (1964), as indicated in equations 1 and 2, below.

$$j = \frac{\eta_0 . \hbar_{ext} Pr_{air}^{2/3}}{\rho_{air} . V_{air} . c_{p,air}} \tag{1}$$

$$\eta_0 . \hbar_{ext} = \left(\frac{A_{total}}{UA} - \frac{A_{total}}{\hbar_{int} . A_{int}} \right)^{-1} \tag{2}$$

The internal convection coefficient was calculated by the correlation proposed by Gnielinski (1976), as a function of the Nusselt number, which, in turn, is a function of the friction factor. The friction factor was calculated through the Shah and Sekulic (2003) correlation for laminar flow, and Bhatti and Shah (1987) for the transition/turbulent flows.

2.3.2 Pressure drop

The air-side pressure drop was measured by a differential pressure transducer installed at inlet and outlet of the heat exchanger, which allowed the calculation of the air-side friction factor, as follows:

$$f = \frac{A_{min}}{A_{total}} \frac{\rho_{air}}{\rho_{air,in}} \left\{ \frac{2 . \Delta P_{air} \rho_{air,in}}{G_{air,max}^2} - \left(\frac{\rho_{air,in}}{\rho_{air,out}} - 1 \right) \left(1 + \frac{A_{min}^2}{A_f^2} \right) \right\} \tag{3}$$

2.4 Samples characterization

As previously mentioned, the samples were characterized in terms of heat transfer and pressure drop. Figure 2a shows the behavior of the overall thermal conductance coefficient as a function of volumetric airflow rate for all samples. As expected, the UA increases as the airflow rate increases and the condensers with the largest external heat transfer area presented the higher overall thermal conductance coefficient. Considering that the measurement uncertainty of this parameter is of the order of ± 9%, it was observed that the performance of the samples (#1 and #2), (#3 and #4) and (#5 and #6) is practically the same regardless of the number or shape of the microchannels. In other words, the heat transfer rate is not significantly affected by the internal convection coefficient in these heat exchangers. However, differences of up to 28% in the overall thermal conductance were found between samples #7 and #8, indicating that the number and shape of the microchannels is relevant when the heat exchanger has a larger heat transfer area. A larger heat transfer area means a higher heat transfer rate, which in turn means a higher mass flow rate on the water side and, consequently, a change in flow patterns, especially in the condenser #7, with smaller channels.

Colburn factor *j* for samples #8, #9 and #10 is shown in Figure 2b as a function of the Reynolds number ($Re_{Lp} = \rho . Q . L_{louver} / A_{min} \mu$)). As expected, the Colburn factor *j* varies inversely and linearly with the Reynolds number. The observed differences are due to the variations in geometry, notably number of fins, number of passes and face area.

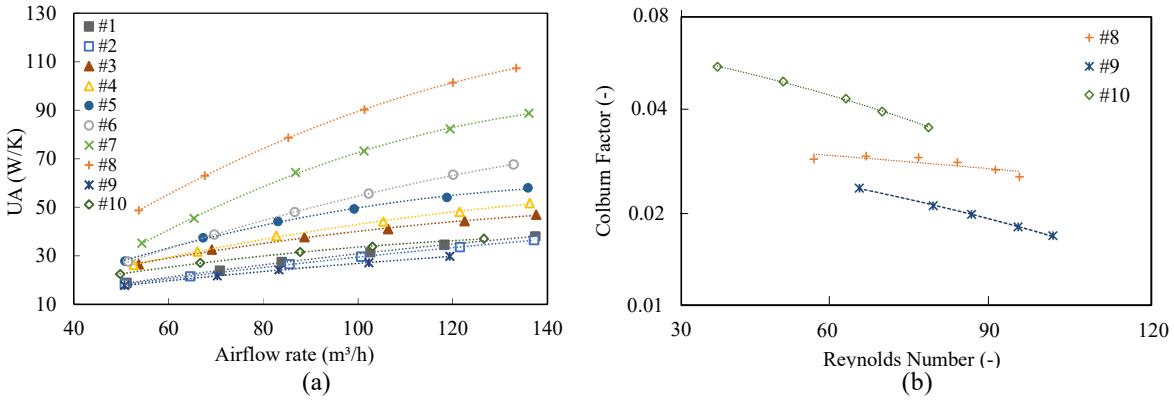

Figure 2: (a) Overall thermal conductance coefficient and (b) Colburn factor *j*

The air-side pressure drop was obtained from the static pressure measurements at the inlet and outlet of the heat exchanger. Figure 3a shows the pressure drop as a function of the airflow rate for all condensers tested. As expected, the pressure drop is a quadratic function of the airflow rate. It is worth noting that the pressure drop increases as the face area of the heat exchanger decreases. The pressure drop in samples #1 and #4, both with small face area, for example, is so high that it hinders the use of these heat exchangers in domestic refrigeration application. In contrast, the pressure drop in samples #9 and #10 are low enough to successfully be used in such application.

The friction factor *f* as a function of the Reynolds number is shown in Figure 3b. Similar to the Colburn factor *j*, an inverse linear behavior between these parameters is observed. Again, it is noted that the shift between curves are due to the variation in the geometry of the heat exchangers. Moreover, the heat exchangers #9 and #10, despite of similar pressure drop, present distinguished friction factor. This is due to the smaller minimum area of the condenser #9, because of the presence of the two vertical headers.

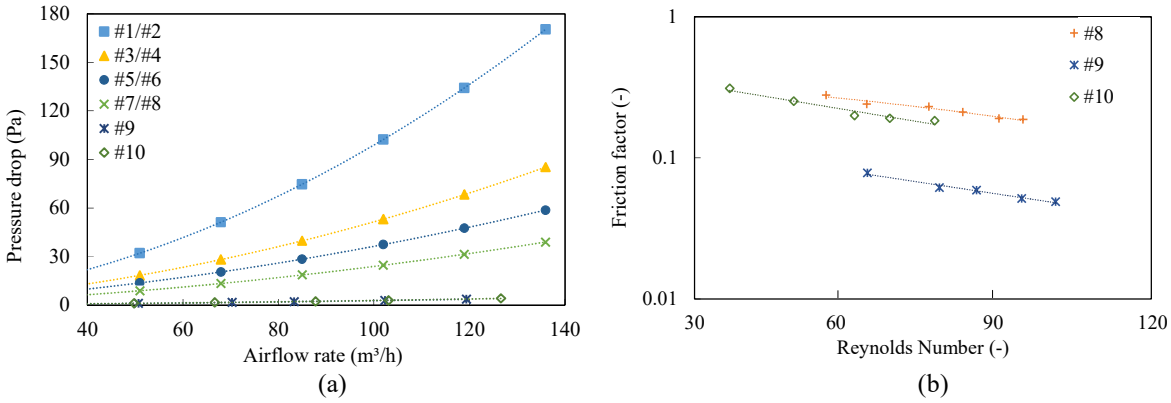

Figure 3: (a) Pressure drop (b) Friction factor *f*

2.5 Household refrigerator

A french-door bottom-mount frost-free refrigerator, with a 166-liter freezer compartment placed below a 374-liter fresh food compartment was used. The refrigeration system is comprised by a reciprocating compressor, a forced-draft wire-and-tube condenser and a finned-tube evaporator. The system is charged with 51g of R600a (isobutane).

As previously mentioned, some condensers samples were installed in the household refrigerator to evaluate the system performance as well as to generate data for the validation of the refrigeration simulation platform, later explored in this work. The samples were selected based on its overall thermal conductance and pressure drop. Special attention was given to the pressure drop, since the original airflow system, including the fan, was not modified. Measurements were performed to identify the fan performance and the impedance curves of the airflow system, following recommendations by Knabben *et al.* (2014). Figure 4 shows the operating point of the system with all the condensers, including the refrigerator's original one, a compact forced-draft wire-on-tube (WOT) type. Based on these data, the

samples #7 to #10 were selected to be evaluated at the refrigerator. Note that the operating points of samples #9 and #10 are similar to the one obtained with the original condenser and that samples #7 and #8 presented a substantial drop on airflow rate due to the higher air-side pressure drop caused by higher fins density.

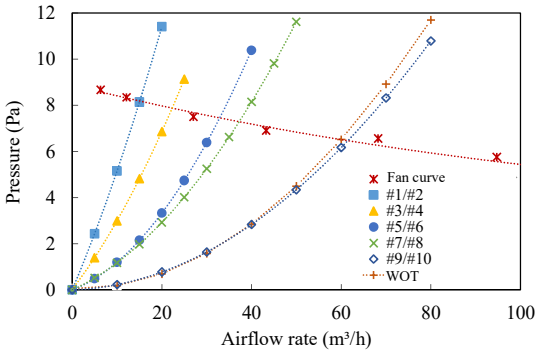

Figure 4: Airflow system operating points

Standardized energy consumption tests were performed according to the ISO 15502 (2005) Standard. The original control strategy of the refrigerator was kept constant during the tests. Table 2 shows the energy consumption, the overall thermal conductance, the airflow rate, the refrigerant mass flow rate and other relevant parameters.

Table 2: Energy consumption results

Samples	**WOT**	**#7**	**#8**	**#9**	**#10**
Energy consumption (kWh/month)	75.9	77.2	75.3	71.6	71.4
UA (W/°C)	7.1	15.9	29.7	20.0	25.8
Airflow rate (m³/h)	60.0	37.2	37.2	61.5	61.5
Compressor discharge temperature (°C)	57.5	61.8	59.0	55.2	54.6
Condenser inlet temperature (°C)	46.3	50.6	47.7	40.2	41.0
Condenser outlet temperature (°C)	44.8	40.2	41.0	38.6	37.3
Subcooling degree (°C)	3.7	3.2	3.0	2.5	2.6
Refrigerant mass flow rate (kg/h)	2.33	2.27	2.36	2.50	2.45
Refrigerant charge (g)	58.0	51.2	57.4	65.9	57.0

It is worth noting that the condensers #9 and #10 lead to a reduction of an approximately 7% drop in energy consumption, when compared to the original wire-on-tube condenser. It was also noted that the replacement of the original condenser by the condenser #8 did not cause any substantial changes in performance, regardless of the considerable higher UA. Moreover, condenser #7 presented an increase of 1.7% in energy consumption.

Table 2 also shows the average compressor discharge and inlet/outlet condenser temperatures during an on-cycle of an energy consumption test. Note that those temperatures are substantially lower when condensers #9 and #10 are in place, which explains the lower energy consumption values. Moreover, among all the samples, condenser #7 presented the highest inlet condenser temperature and the lowest refrigerant mass flow rate, possibly due to the greatest refrigerant-side pressure drop.

3. NUMERICAL APPROACH

The numerical approach involved (i) the development of a mathematical model for serpentine-type microchannel condensers and (ii) the conflation of such model with an in-house refrigerator simulation platform for domestic refrigerators (Gonçalves *et al.*, 2008, Hermes *et al.*, 2009). Both models were appropriately validated with experimental data obtained in the wind tunnel and in the climatic chamber.

3.1 Microchannel Condenser Numerical Model

The condenser model was developed based on the discretization of the serpentine in small control volumes using a two-dimensional mesh in order to predict the refrigerant state, the temperature distribution and the pressure drop along

the heat exchanger. The model was divided into two submodels: (i) thermal and (ii) hydrodynamic submodel, which provides the heat transfer rate and the pressure drop as an outcome, respectively.

3.1.1 Thermal submodel

Some simplifying assumptions were assumed: (i) steady-state regime, (ii) one-dimensional airflow rate, (iii) uniform air and refrigerant distribution, (iv) fully developed refrigerant flow, (v) microchannels and fins with constant cross section, (vi) uniformly distributed fins, (vii) negligible kinetic and potential energy variations (viii) uniform control volume wall temperature and (ix) no conduction on the tube wall.

The condenser operation is characterized by three distinct regions: (i) superheating, (ii) condensation and (iii) subcooling. Latent heat transfer occurs at the condensation region, while sensible heat transfer characterizes both other regions. Energy balances are performed in each region, both on the refrigerant and air sides. Since the fluid state at the control volumes outlet is unknown, the ε-NTU method was chosen to model the heat transfer process. The internal convection coefficient in the two-phase region was calculated by the correlation proposed by Kim and Mudawar (2013), while the correlation proposed by Adams *et al.* (1998) was used for both monophasic regions.

The external convection coefficient was obtained from equation 1. However, none of the available Colburn factor correlations found in the literature (Dong *et al.,* 2007; Chang and Wang, 1996; Chang and Wang, 1997; Kim and Bullard, 2002; Li and Wang, 2010; and Sunden and Svantesson, 1992) were able to reproduce appropriately the experimental results obtained with samples #1 to #8, as shown in Figure 5a. Thus, it was decided to develop a specific correlation for these heat exchangers, which is valid for the ranges $53 \leq Re_{Lp} \leq 524$ and $7.58 \leq F_a \leq 7.91$, as follows:

$$j = 7.10^{-9}.Re_{Lp}^{-0.36944}.F_a^{8.04455} \quad (4)$$

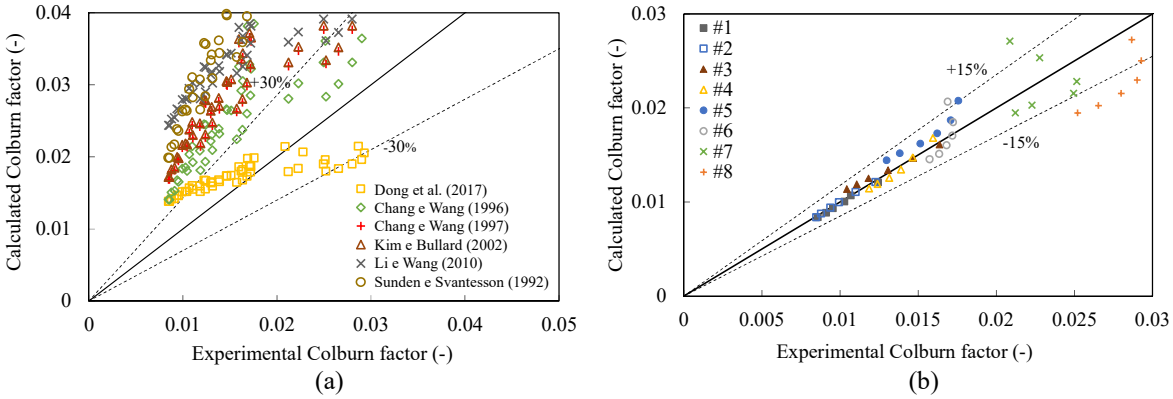

Figure 5: (a) Experimental Colburn factor *vs.* literature correlations (b) Proposed correlation *vs.* experimental data

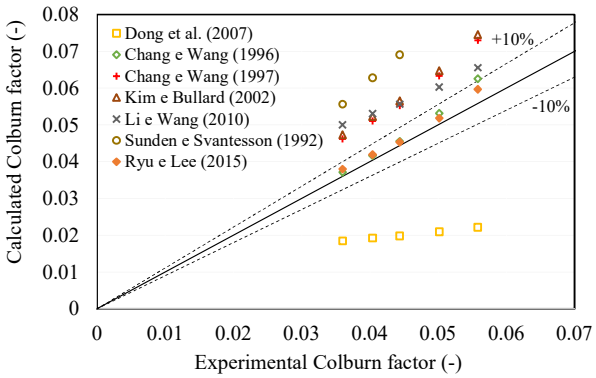

Figure 6: Experimental Colburn factor *vs.* literature correlations for condenser #10

Figure 5b shows that the proposed correlation predicts reasonably well the experimental data with 85% of the data within a ±15% error band. Samples #7 and #8 lays slightly out probably due to the change in flow patterns, as previously mentioned.

Similarly, correlations for condenser #10, which has a distinct fin density from that of the condensers #1 to #8, were deployed to predict the external convection coefficient. In this case, it was observed that the correlations of Chang and Wang (1997) and Ryu and Lee (2015) reasonably correlate the experimental data inside an error band of the order of ±10% (see Figure 6). The latter correlation was selected, which is valid in the 100 ≤ ReLp ≤ 3000 range. It is worth noting that the developed model is not suitable for condensers with vertical headers and, therefore, correlations for the condenser #9 were not investigated.

3.1.2 Hydrodynamic submodel

The friction factor parameter was derived from static pressure measurements in samples #1 to #8 and compared with correlations in the literature (Chang et al. (2007), Chang and Wang (1997), Kim and Bullard (2002) and Li et al. Wang (2010)). As shown in Figure 7a, none of the correlations was able to adequately reproduce the experimental data. Thus, a new correlation was developed, valid for samples #1 to #8 at the same range of application of equation (4).

$$f = 8{,}46.10^{-7}.Re_{Lp}^{-0{,}661596}.F_a^{7{,}295737} \quad (5)$$

Figure 7b shows that the proposed correlation agrees reasonably well with the experimental data and that 90% of the points fell within a ±15% error band.

Similarly, a correlation of the literature was identified to predict the friction factor for condenser #10. As shown in Figure 8, the correlation proposed by Kim and Bullard (2002), with an application range of 100 ≤ Re_{Lp} ≤ 600, satisfactorily reproduces the experimental data with maximum deviations of ±20%.

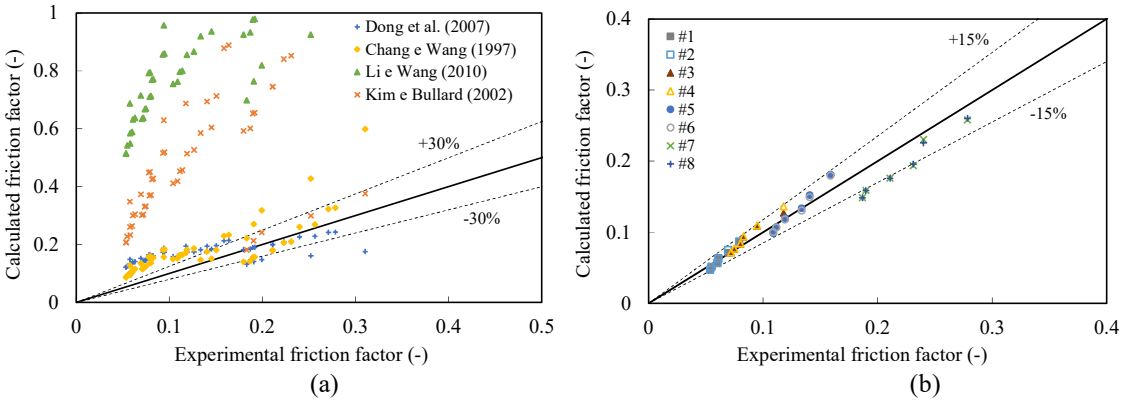

Figure 7: (a) Experimental friction factor *vs.* literature correlations (b) Proposed correlation *vs.* experimental data

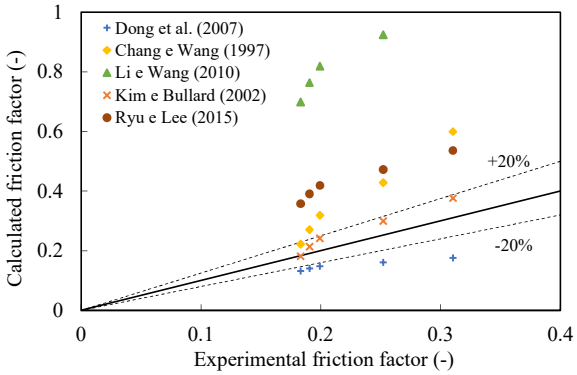

Figure 8: Friction factor *vs.* literature correlations for condenser #10

3.2 Refrigerator simulation platform

As shown previously, the model proposed by Gonçalves *et al.* (2008) and Hermes *et al.* (2009) was extended to allow the simulation of household refrigerators mounted with microchannel forced-draft condensers. Thus, it became possible to estimate the effect of the condenser geometry on the energy consumption of the appliance. To do so, the proposed model was validated.

The model validation was performed with the original wire-on-tube condenser as well as the condensers #7, #8 and #10. Table 3 compares the model prediction with the experimental values of energy consumption (EC), compressor run time ratio (RTR) and compressor power (W_K). Note that the model can reasonably predict the experimental data with a maximum deviation of ±3.5% in energy consumption. The energy consumption estimate for condenser #7 was hindered due to the model difficulty to predict the pressure drop on the refrigerant side, which is higher for that specific sample.

Table 3: Simulation platform validation

		Experimental	Model	Error (%)
WOT	EC (kWh/month)	75.9	73.9	2.6
	RTR (-)	0.63	0.62	2.3
	WK (W)	135.0	142.1	5.3
#10	EC (kWh/month)	71.4	70.8	0.9
	RTR (-)	0.57	0.6	4.6
	WK (W)	139.0	139.4	0.3

		Experimental	Model	Error (%)
#7	EC (kWh/month)	77.3	74.8	3.3
	RTR (-)	0.65	0.62	5.4
	WK (W)	138.0	142.8	3.5
#8	EC (kWh/month)	75.3	74.4	1.1
	RTR (-)	0.62	0.62	0.8
	WK (W)	135.0	142.5	5.5

3.3 Parametric study: Refrigerator performance

Once the model is validated, it was used to find an optimum condenser geometry through a parametric study, considering the energy consumption as an outcome. Three parameters were evaluated: (i) fins density (from 100/m to 700/m), (ii) condenser depth (from 12mm to 102mm) and (iii) number of passes (from 16 to 20). All other geometric parameters were kept constant and identical to the sample #10. It must be mentioned that the number of microchannel ports increases linearly with the condenser depth, in a ratio of 1.7/mm.

Table 4 presents the energy consumption results in kWh/month for all simulated configurations. The blank cells represent situations of lack or excess of heat exchange area, when the model suffers with convergence issues.

Table 4: Energy consumption [kWh/month] *vs.* microchannel condenser geometry

Depth (mm)	16 passes							18 passes							20 passes						
	Fins density (-/m)							Fins density (-/m)							Fins density (-/m)						
	100	200	300	400	500	600	700	100	200	300	400	500	600	700	100	200	300	400	500	600	700
12	-	-	-	75.9	73.3	71.9	71.4	-	-	-	75.1	72.6	71.3	70.8	-	-	78.7	74.4	72.1	70.9	70.3
17	-	-	74.6	71.7	70.4	70.1	70.7	-	-	73.8	71.1	68.8	69.4	70.8	-	-	73.2	70.5	69.3	68.9	69.2
22	-	76.7	71.6	69.8	69.4	69.9	71.7	-	75.8	70.9	69.2	68.6	69.2	69.9	-	75.0	70.4	68.8	68.3	68.5	69.8
27	-	73.6	69.9	69.0	69.4	70.7	73.8	-	72.9	69.3	68.4	69.0	69.7	70.6	-	72.2	68.9	67.9	68.0	68.9	71.2
32	-	71.6	69.0	68.7	69.9	72.1	76.6	-	71.0	68.4	68.1	69.4	70.9	72.4	-	70.4	68.0	67.6	68.3	69.9	73.4
37	-	70.3	68.4	68.8	70.8	74.0	80.2	-	69.7	67.9	68.1	69.7	73.6	74.8	-	69.2	67.5	67.5	68.9	71.3	76.0
42	-	69.3	68.2	69.2	72.0	76.3	84.3	-	68.8	67.7	68.4	70.8	75.8	77.8	-	68.4	67.2	67.8	69.3	73.1	-
47	-	68.7	68.2	69.9	73.6	79.1	-	-	68.2	67.6	68.9	72.1	78.5	-	-	67.8	67.1	68.2	69.8	75.1	-
52	-	68.3	68.4	70.7	-	-	-	-	67.8	67.7	69.7	73.7	79.5	-	-	67.4	67.2	68.8	70.9	77.4	-
57	-	68.0	68.7	71.8	-	-	-	-	67.5	67.9	70.5	-	-	-	-	67.1	67.3	69.5	73.0	-	-
62	-	67.8	69.1	73.7	-	-	-	72.5	67.3	68.3	71.5	-	-	-	72.0	66.9	67.6	70.4	75.2	-	-
67	72.5	67.7	69.7	75.6	-	-	-	71.8	67.2	68.7	72.7	-	-	-	71.2	66.8	68.0	-	79.2	-	-
72	71.7	67.7	70.3	76.4	-	-	-	71.0	67.2	69.0	73.9	-	-	-	70.5	66.7	-	-	-	-	-
77	71.0	67.7	70.9	77.1	-	-	-	70.4	67.1	-	-	-	-	-	69.9	66.7	-	-	-	-	-
82	70.5	67.8	71.6	78.7	-	-	-	69.9	67.2	-	-	-	-	-	69.4	66.7	-	-	-	-	-
87	70.0	67.9	73.0	-	-	-	-	69.4	67.3	-	-	-	-	-	69.0	66.7	-	-	-	-	-
92	69.6	68.1	74.3	-	-	-	-	69.0	67.4	-	-	-	-	-	68.6	66.8	-	-	-	-	-
97	69.3	68.3	75.6	-	-	-	-	68.7	67.5	-	-	-	-	-	68.3	-	-	-	-	-	-
102	69.0	68.5	76.7	-	-	-	-	68.4	-	-	-	-	-	-	68.0	-	-	-	-	-	-

The increase of the fins density or the condenser depth causes an increase in the total heat transfer area. In contrast, the air-side pressure drop also raises, overloading the airflow system and consequently decreasing the total airflow rate, leading to a tradeoff situation. In other words, for a constant depth, there is an optimum fins density that minimizes energy consumption, and vice versa. As regards as the number of passes, it is clear that, for identical geometries, the increase of the number of passes decreases the energy consumption, since there is an increase of the total heat transfer area without a substantial overload of the airflow system. It must be mentioned that the number of passes was limited to 20 due to the space available in the compressor niche.

A brief inspection of Table 3 shows that the configuration with fins density of 200/m, 20 passes and 72mm depth presents the lowest energy consumption (66.7 kWh/month), 13% less than that of the original configuration.

4. CONCLUDING REMARKS

The aim of this work was to investigate the effect of microchannel condensers in a specific household refrigerator model. To this end, a mathematical model was developed and validated with experimental data obtained in a wind tunnel. The heat transfer rate and pressure drop model predictions fell within an error band of ± 10% and ± 20%, respectively. Such model was incorporated into an existing domestic refrigerator simulation platform, allowing the study of the impact of the microchannel condensers geometry on the energy consumption of the refrigerator. Validation against experimental data was also performed and maximum deviations of ± 3.5% were observed in the energy consumption. It was also found that condensers #9 and #10 caused a 7% drop in energy consumption compared to the original wire-on-tube condenser. Finally, the microchannel condenser geometry was optimized for the refrigerator model in order to minimize the energy consumption. A condenser with 20 passes, 200mm height, 180mm width, 72mm depth, 200 fins/meter and 46 rectangular channels of 1.2mm of hydraulic diameter, results in an energy consumption 13% lower than that obtained with the original wire-on-tube condenser. Indeed, microchannel forced-draft condensers have a great potential to be successfully used in household refrigerators in the near future.

NOMENCLATURE

A	area	m^2
A_{coil}	coil surface area	m^2
A_f	face area	m^2
A_{min}	minimum area	m^2
A_{total}	total heat transfer area	m^2
c_p	specific heat,	J/(kgK)
F_a	Finning factor	-
G	mass flux	$kg/(m^2s)$
h	heat transfer coefficient	W/(m°C)
L_{louver}	louver length	m
P	pressure	Pa
Pr	Prandtl number	-
Q	volumetric airflow rate	m^3/s
Re_{Lp}	Reynolds number (louver base)	-
v	velocity	m/s
Greek symbols		
η_0	fins efficiency	-
ρ	density	kg/m^3
μ	dynamic viscosity	Pa.s
Θ	louver angle	degree
Subscript		
air	air	
ext	external	
in	inlet	
int	internal	
max	maximum	
out	outlet	

REFERENCES

Adams, T.; Abdel-Khalik, S.; Jeter, S.; Qureshi, Z; 1998; An experimental investigation of single-phase forced convection in microchannels. International Journal of Heat and Mass Transfer, v. 41, n. 6, p. 851 – 857.

ASHRAE Standard 37; 1988: Methods of testing for rating electrically driven unitary air-conditioning and heat pump equipment. [S.l.].

ASHRAE Standard 41.2; 1987: Standard methods for laboratory airflow measurement. [S.l.].

ASHRAE Standard 51; 1999: Laboratory methods of testing fans for aerodynamic performance rating. [S.l.].

Bhatti, S. M.; Shah, R. K.; 1987; Turbulent and transition convective heat transfer in ducts. Handbook of Single-Phase Convective Heat Transfer.

Chang, Y.-J.; wang, C.-C.; 1996; Air side performance of brazed aluminum heat exchangers. Journal of Enhanced Heat Transfer, v. 3, p.15-28.

Chang, Y.-J.; wang, C.-C.; 1997; A generalized heat transfer correlation for Iouver fin geometry. International Journal of Heat and Mass Transfer, v. 40, n. 3, p.533–544.

Colburn, A. P.; 1964; A method of correlating forced convection heat-transfer data and a comparison with fluid friction. International Journal of Heat and Mass Transfer, v. 7, n. 12, p. 1359 – 1384.

Dong, J.; Chen, J.; Chen, Z.; Zhang, W.; Zhou, Y.; 2007; Heat transfer and pressure drop correlations for the multi-louvered fin compact heat exchangers.

Gnielinski, V.; 1976; New equations for heat and mass transfer in turbulent pipe and channels flow. International Chemical Engineer, v. 16, p. 359–368.

Gonçalves, J. M.; Hermes, C. J. L.; Melo, C.; Knabben, F. T.; 2008; A Simplified Steady-State Model for Predicting the Energy Consumption of Household Refrigerators and Freezers.

Hermes, C. J.; Melo, C.; Knabben, F. T.; Gonçalves, J. M.; 2009; Prediction of the energy consumption of household refrigerators and freezers via steady-state simulation. Applied Energy, v. 86, n. 7–8, p. 1311 – 1319.

Huang, L.; Lee, M. S.; Saled, K., Aute, V., Radermacher, R.; 2014; A computational fluid dynamics and effectiveness-NTU based co-simulation approach for flow mal-distribution analysis in microchannel heat exchanger headers. ATE, v. 65, p. 447–457.

Incropera, F.; Bergman, T.; Dewitt, D.; Lavine, A.; 2007; Fundamentals of Heat and Mass Transfer. [S.l.]: Wiley.

ISO 15502; 2005: Household refrigerating appliances - Characteristics and test methods. [S.l.].

Kim, M. -H; Bullard, C. W.; 2002; Air-side thermal hydraulic performance of multi-louvered fin aluminum heat exchangers. IJR, v. 25, n. 3, p. 390-400.

Kim, S. M.; Mudawar, I.; 2013; Universal approach to predicting heat transfer coefficient for condensing mini/micro-channel flow. International Journal of Heat and Mass Transfer, v. 56, n. 1-2, p. 238–250.

Knabben, F. T.; Melo, C.; Vieira, L. A.; Hartmann,; 2014; D. Fluid dynamic characterization of the cold air loop of household refrigerators. 15th Brazilian Congress of Thermal Sciences and Engineering November, n. 1999.

Li, W.; Wang, X.; 2010; Heat transfer and pressure drop correlations for compact heat exchangers with multi-region louver fins. International Journal of Heat and Mass Transfer, v. 53, n. 15-16, p. 2955–2962.

Park, C. Y.; Hrnjak, P.; 2008; Experimental and numerical study on microchannel and round-tube condensers in a R410A residential air-conditioning system. International Journal of Refrigeration, v. 31, n. 5, p. 822–831.

Ryu, K.; Lee, K.-S.; 2015; Generalized heat-transfer and fluid-flow correlations for corrugated louvered fins. International Journal of Heat and Mass Transfer, v. 83, p. 604 – 612.

Shah, R. K.; Sekulic, D. P.; 2003; Fundamentals of Heat Exchanger Design. [S.l.]: John Wiley & Sons, Inc., Hoboken, New Jersey v. 83.

Shao, L.-l.; Yang, L.; Zhang, C.-l.; Gu, B.; 2009; Numerical modeling of serpentine microchannel condensers. International Journal of Refrigeration, v. 32, n. 6, p. 1162–1172.

Sunden, B.; Svantesson, J.; 1992; Correlation of j- and f- factors for multilouvered heat transfer surfaces. Proceedings of the 3rd UK National Heat Transfer Conference, p. 805–811.

ACKNOWLEDGEMENTS

This study was made possible through the financial investment from the EMBRAPII Program (POLO/UFSC EMBRAPII Unit - Emerging Technologies in Cooling and Thermophysics). The authors thank Whirlpool Latin America S.A. for financial and technical support.